Observation of bandgap guidance of optical vortices in a tunable negative defect

Article *in* Optics Letters · June 2010

DOI: 10.1364/OL.35.002106 · Source: PubMed

Observation of bandgap guidance of optical vortices in a tunable negative defect

Daohong Song,[1] Xiaosheng Wang,[2,3] Daniel Shuldman,[2] Jiandong Wang,[4] Liqin Tang,[1] Cibo Lou,[1] Jingjun Xu,[1] Jianke Yang,[5] and Zhigang Chen[1,2,*]

[1]*The Key Laboratory of Weak-Light Nonlinear Photonics, Ministry of Education and TEDA Applied Physics School, Nankai University, Tianjin 300457, China*

[2]*Department of Physics and Astronomy, San Francisco State University, San Francisco, California 94132, USA*

[3]*Department of Physics, University of Cincinnati, Cincinnati, Ohio 45221, USA*

[4]*College of Physical Electronics, University of Electronic Science & Technology of China, Chengdu 610054, China*

[5]*Department of Mathematics and Statistics, University of Vermont, Burlington, Vermont 05401, USA*

**Corresponding author: zhigang@sfsu.edu*

Received March 12, 2010; revised May 28, 2010; accepted June 1, 2010;
posted June 3, 2010 (Doc. ID 125310); published June 14, 2010

We experimentally demonstrate linear bandgap guidance of optical vortices as high-gap defect modes (DMs) in two-dimensional induced photonic lattices. We show that donut-shaped vortex beams can be guided in a tunable negative (lower-index) defect, provided that the defect strength is set at an appropriate level. Such vortex DMs have fine features in the "tails" associated with the lattice anisotropy and can be considered as a superposition of dipole DMs. Our numerical results find good agreement with experimental observations. © 2010 Optical Society of America

OCIS codes: 190.4420, 160.5293.

Light propagation in periodic materials has attracted a great deal of interest. In the spatial domain, much of the work has focused on nonlinear localization of light into discrete or gap solitons in waveguide arrays [1,2]. Recently, linear localization of light due to spatial bandgap guidance, namely, *linear defect modes* (DMs), has also been studied. In particular, one-dimensional and two-dimensional (2D) linear DMs were predicted and investigated experimentally in induced photonic lattices and laser-written waveguide arrays [3–11]. It has also been suggested that linear control of beam propagation and multicolor routing can be realized with spatial photonic DMs [12]. However, thus far only fundamental linear DMs have been observed with a Gaussian beam excitation. It is of great interest and an experimental challenge to demonstrate PCF-like guidance of dipole and vortex modes.

In this Letter, we study experimentally linear propagation of a singly charged vortex beam through a tunable negative defect optically induced in a 2D photonic lattice. We show that the vortex beam can be guided in the defect as a DM, provided that the defect is not too deep. The vortex maintains the donut shape and vortex singularity at the defect site, but its "tails" contain fine features of additional vortex pairs along the principal axes of the square lattice. This vortex mode is identified as a high-gap DM, in perfect agreement with our earlier prediction [7]. In addition, we find that the fine features can be explained from the anisotropy of the induced lattices, and the vortex DMs can be viewed as a superposition of dipole modes also observed in our experiment. These experimental results are corroborated by numerical simulations.

The experiment setup is similar to that used in our demonstration of 2D fundamental DMs [8], except that now we have two sets of photonic lattices for tuning the defect strength, and the probe beam is a singly charged vortex beam [Fig. 1(a)]. A laser beam ($\lambda = 488$ nm) splits through a polarizing beam splitter before entering a biased strontium barium niobate photorefractive crystal. The ordinarily polarized beam splits again into two lattice-inducing beams: one has an uniform periodic intensity pattern, as shown in Fig. 1(c) [peak intensity I_c], and the other has a zero-intensity defect site on otherwise uniform periodic pattern, as shown in Fig. 1(d) [peak intensity I_d]. Superimposing the two lattice-inducing beams of equal lattice spacing results in a nonzero but tunable defect [an example obtained at $I_d/I_c = 1/2$ is shown in Fig. 1(b)]. The tunability of the defect strength is realized by varying the intensity ratio I_d/I_c (e.g., at $I_d/I_c \gg 1$, the defect is deep or close to zero intensity, but at $I_d/I_c \ll 1$, the defect is shallow or close to washout). With a positive voltage, the crystal turns into a self-focusing medium, and the two beams induce a 2D photonic lattice with a single-site *negative* defect [8]. The extraordinarily polarized beam passes through a vortex mask, and its intensity is kept sufficiently low so that the vortex beam undergoes linear propagation through the defect channel. When needed, an interferometer is employed to measure the phase structure of the vortex beam exiting the crystal. (Interference

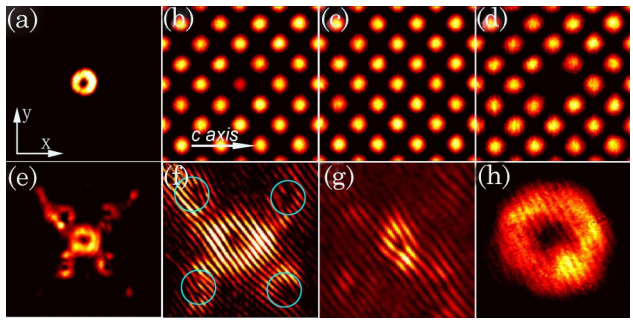

Fig. 1. (Color online) Experimental results of bandgap guidance of a vortex beam in a tunable negative defect. (a) Vortex at input. (b)–(d) Induced lattices with nonzero-intensity defect, no defect, and zero-intensity defect, respectively. (e), (f) Vortex output from the defect in (b) and its zoom-in interferogam. The circles in (f) mark the location of the vortex pairs. (g) Interferogram when the vortex is excited at nondefect site. (h) Vortex diffraction output when lattice is absent.

between the vortex and a tilted plane wave results in "fork fringes" in the interferogram, representing phase singularity.)

Typical experimental results are presented in the bottom panels of Fig. 1. Under proper experimental conditions, the input vortex beam (20 μm in diameter) is guided into the defect channel [Fig. 1(e)], maintaining a donut-shaped pattern in the defect site with "tails" extending along two principal axes of the square lattice. The propagation length is the crystal length of 1 cm, corresponding to about a 6 diffraction length. This result was obtained at 42 μm lattice spacing, 2.3 kV/cm bias field, and $I_d/I_c = 1/2$. For comparison, the same vortex beam diffracts dramatically when the defect/lattice is removed [Fig. 1(h)], showing no self-action of the vortex beam under the same bias condition. Fine features can be seen in the interferogram obtained by interference between the output vortex beam and an inclined broad beam (quasi-plane wave): while the phase singularity is maintained in the vortex center [Fig. 1(f)], additional vortex pairs are evident along the four "tails" away from the defect site, manifested by two close but separated fork fringes in the interferogram of Fig. 1(f). These fine structures in the "tails," as elaborated below, provide us a way to identify the properties of the vortex DMs. By comparing with the theoretical results [7], it is apparent that the input singly charged vortex beam has evolved into a high-gap DM, whose propagation constant resides between the second and third Bloch bands. We emphasize that the localization of the vortex beam arises from the linear bandgap guidance, quite different from stationary propagation of second-band vortex solitons where the vortex beam itself creates a *positive* defect with self-focusing nonlinearity [13]. For comparison, the interferogram from the vortex beam exiting a normal lattice site is shown in Fig. 1(g), where a single vortex (instead of vortex pair) is observed along each "tail."

The formation of the vortex DMs depends on the defect strength [7]. A series of experiments is performed to illustrate the influence of the defect strength. To do so, we keep the bias field and I_c fixed but tune the defect strength by gradually varying I_d. We found that the vortex can be guided only when the defect is not too deep (or the intensity in the defect site is not close to zero). Examples of varying the intensity ratio I_d/I_c or the bias field (both control the induced index change at the defect site) are shown in Fig. 2. When the biased field is set at 2.6 kV/cm, guidance of the vortex beam is clearly observed at $I_d/I_c = 1$ [Fig. 2(a)] (which corresponds to a half-intensity defect). However, once the uniform lattice beam is removed ($I_c = 0$), the vortex beam cannot be confined in the defect site under the same bias condition [Fig. 2(b)]. At this zero-intensity defect, the vortex DM cannot form, even at a decreased bias field of 1.4 kV/cm [Fig. 2(c)] or an increased bias field of 3.2 kV/cm [Fig. 2(d)]. Thus, bandgap guidance of the vortex clearly occurs in the half-intensity defect, but deteriorates in the zero-intensity defect. There might be a threshold for the defect strength that would support the vortex DM, but, experimentally, it is difficult to determine such a threshold. Nevertheless, these observations agree well with the theoretical prediction [7]. Intuitively, a negative defect supports a DM in the photonic bandgap. When the defect gets deeper, the propagation constant of the DM moves deeper toward a higher bandgap. Because of the limited number of fully opened higher gaps, the propagation constant of the DM may move into a higher Bloch band, and, eventually, localized DMs disappear.

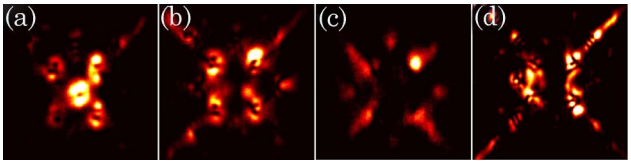

Fig. 2. (Color online) Output of the vortex beam through (a) a half-intensity ($I_d/I_c = 1$) defect and (b) a zero-intensity defect at a fixed bias field of 2.6 kV/cm. (c), (d) Output of the vortex beam through the zero-intensity defect when the bias field is decreased to 1.4 kV/cm and increased to 3.2 kV/cm, respectively.

The above observations are corroborated by numerical solutions [7] and BPM simulations with a 2D continuum model used in [12]. Numerical solution of the vortex DM is shown in Fig. 3(a), and beam propagation results obtained with parameters close to those from the experiment are shown in Fig. 3(b). An input vortex beam [Fig. 3(d), top] is guided in a negative half-intensity defect ($I_d/I_c = 1$), as shown in Fig. 3(b), but couples dramatically into surrounding lattice sites for a zero-intensity defect [Fig. 3(d), bottom], in agreement with the experimental results of Figs. 2(a) and 2(b). A subtle but interesting feature merits discussion when one carefully compares the vortex singularities in the "tails" obtained from numerical solution, BPM simulation, and experiment. In the solution [Fig. 3(a), bottom] and numerical simulation [Fig. 3(b), bottom], the vortex pairs in all "tails" have opposite topological charges as compared with that of the main vortex in the center. This can be seen either by tracing the round-trip phase variation or the directions of fringe bifurcation (forking). However, from the experimental results of Fig. 1(g), the vortex pairs in one direction have the opposite topological charge, but those in the other orthogonal direction have the same charge with respect to the charge of the center vortex. We mention that a similar phenomenon was also observed for higher gap fundamental DMs [8]. Here the difference seems to result from the anisotropy of the induced

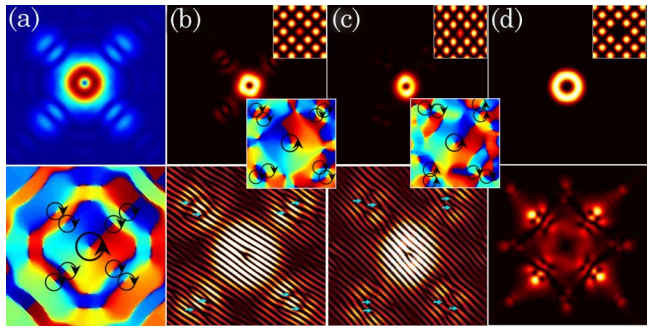

Fig. 3. (Color online) Numerical results of the vortex DM: (a) DM solution (top) and its phase structure (bottom); (b), (c) intensity (top) and interferogram (bottom) of output vortex after 1 cm of propagation through lattice with a half-intensity defect; (d) input vortex (top) and its output (bottom) from a zero-intensity defect. The insets in (b)–(d) show the corresponding lattices and DM phase structure. Result (c) is from an anisotropic lattice.

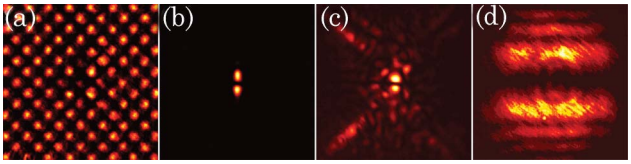

Fig. 4. (Color online) Experimental results of linear guidance of a dipole beam in a negative defect: (a) Induced lattice with defects, (b) input dipole beam, (c) guidance of the dipole beam in the central defect, (d) normal diffraction of dipole beam when the lattice is removed after 2 cm linear propagation at a bias field of 1.9 kV/cm.

lattices (i.e., the couplings between waveguides along the x and y directions are slightly different) owing to the anisotropic photorefractive nonlinearity [14,15]. With an anisotropic lattice in the form of $[\cos(\frac{\pi x}{d}) + \cos(\frac{0.8\pi y}{d})]^2$ (d is the lattice spacing), we find by simulation that the vortex beam forms a DM with "tail" structures similar to that from the experimental observation. Results from the anisotropic lattice are shown in Fig. 3(c), where the topological charges of the vortex pairs along one direction are different from those along the orthogonal direction.

As discussed in [7], a vortex DM can be regarded as a superposition of two dipole modes along orthogonal axes with a $\pi/2$ phase delay but the same propagation constant. In fact, dipole DMs have also been observed in our experiment in a similar setting. One example is presented in Fig. 4, where the dipole beam is oriented along the vertical direction. Because of the anisotropy of induced lattices, we find the stability of the dipole DM is sensitive to dipole orientation. In addition, dipole DMs along two lattice principal axes have different propagation constants, and the phase difference between two dipole DMs is expected to change during propagation. Thus, strictly speaking, a vortex mode originating from the superposition of two linear dipole modes cannot be stable in anisotropic lattices, but rather it may break up into dipole modes and undergo charge flipping [15]. In our experiment with the 1-cm-long crystal, the donut-shaped DMs excited with an optical vortex remain robust during linear propagation. We mention that such *linear* vortex DMs are quite different from the *nonlinear* vortex modes found in anisotropic lattices [15–17], where the vortex covers four lattice sites and is localized by the nonlinearity-induced defect. Our single-site vortex tends to break up during nonlinear propagation due to the anisotropic nonlinearity and modulation instability.

In conclusion, we have demonstrated bandgap guidance of optical vortices in photonic lattices with a tunable negative defect. We found that the guidance of the vortex beam in the defect can be realized, provided that the defect is not too deep. The vortex DMs have fine features in the "tails"—better explained from the anisotropy of the induced lattices. Numerical simulation agrees well with the experiment observation. Our results may prove relevant in defect-based light routing [12] and Bragg gratings [18].

This work was supported by the 973 Program (2007CB613203), the National Natural Science Foundation of China (NSFC) (10904078), Program for Changjiang Scholars and Innovative Research Team, the National Science Foundation (NSF), and the U.S. Air Force Office of Scientific Research (USAFOSR).

References

1. H. S. Eisenberg, Y. Silberberg, R. Morandotti, A. R. Boyd, and J. S. Aitchison, Phys. Rev. Lett. **81**, 3383 (1998).
2. J. W. Fleischer, M. Segev, N. K. Efremidis, and D. N. Christodoulides, Nature **422**, 147 (2003).
3. F. Fedele, J. Yang, and Z. Chen, Opt. Lett. **30**, 1506 (2005).
4. F. Fedele, J. Yang, and Z. Chen, Stud. Appl. Math. **115**, 279 (2005).
5. X. Wang, J. Young, Z. Chen, D. Weinstein, and J. Yang, Opt. Express **14**, 7362 (2006).
6. R. Morandotti, H. S. Eisenberg, D. Mandelik, and Y. Silberberg, D. Modotto, M. Sorel, C. R. Stanley, and J. S. Aitchison, Opt. Lett. **28**, 834 (2003).
7. J. Wang, J. Yang, and Z. Chen, Phys. Rev. A **76**, 013828 (2007).
8. I. Makasyuk, Z. Chen, and J. Yang, Phys. Rev. Lett. **96**, 223903 (2006).
9. G. Bartal, O. Cohen, H. Buljan, J. W. Fleischer, O. Manela, and M. Segev, Phys. Rev. Lett. **94**, 163902 (2005).
10. X. Wang, Z. Chen, and J. Yang, Opt. Lett. **31**, 1887 (2006).
11. A. Szameit, Y. V. Kartashov, M. Heinrich, F. Dreisow, T. Pertsch, S. Nolte, A. Tünnermann, F. Lederer, V. A. Vysloukh, and L. Torner, Opt. Lett. **34**, 797 (2009).
12. X. Wang and Z. Chen, Opt. Express **17**, 16927 (2009).
13. G. Bartal, O. Manela, O. Cohen, J. W. Fleischer, and M. Segev, Phys. Rev. Lett. **95**, 053904 (2005).
14. A. Desyatnikov, D. Neshev, Y. Kivshar, N. Sagemerten, D. Träger, J. Jägers, C. Denz, and Y. Kartashov, Opt. Lett. **30**, 869 (2005).
15. A. Bezryadina, J. Young, Z. Chen, D. Neshev, A. Desyatnikov, and Y. Kivshar, Opt. Express **14**, 8317 (2006).
16. P. G. Kevrekidis, D. J. Frantzeskakis, R. Carretero-González, B. A. Malomed, and A. R. Bishop, Phys. Rev. E **72**, 046613 (2005).
17. T. Mayteevarunyooa, B. A. Malomed, B. B. Baizakov, and M. Salerno, Physica D (Amsterdam) **238**, 1439 (2009).
18. N. K. Efremidis and K. Hizanidis, Opt. Express **13**, 10571 (2005).